U. S. DEPARTMENT OF COMMERCE
NATIONAL OCEANIC AND ATMOSPHERIC ADMINISTRATION
NATIONAL WEATHER SERVICE
NATIONAL METEOROLOGICAL CENTER

OFFICE NOTE 81

Damping Properties of the Implicit-Backward Integration Method

Ronald D. McPherson
Development Division

APRIL 1973

DAMPING PROPERTIES OF THE IMPLICIT-BACKWARD INTEGRATION METHOD

I. Introduction

In recent years, considerable attention has been given to the problem of devising optimum methods of utilizing the potentially enormous flow of data from meteorological satellites in operational numerical weather prediction. The unique characteristic of these data is its asynopticity; that is, observations are made not at the standard synoptic times but as the orbiting satellite passes over a particular area of the earth. Such observations are thus distributed both in space and time. Methods for treating data distributed in space have been utilized for many years and are commonly called "objective analysis" methods. With the necessity for incorporating the time dimension, a new phrase has been coined: "four-dimensional data assimilation."

One of the most popular methods of four-dimensional data assimilation, judging by the number of articles appearing in the literature, has been denoted "dynamic" assimilation by Morel and Talagrand (1972). In this approach, the basic vehicle is a prediction model which is integrated more or less continuously, lagging the atmosphere by a few hours in order to allow for communication of observations. As an observation becomes available at a particular point in space and time, the observation is allowed to replace the forecast value at that point. This process is termed "direct insertion." Presumably, if the forecast value is in error, the observation will correct it. The basic concept is that the relationships between mass and motion fields in space and time will be maintained <u>by the model equations</u>.

Direct insertion of an observation (which is not error-free, in general) at a particular point in space and time disturbs the existing relationship of the variables at that point with those at surrounding points. In a primitive-equation model, this disturbance forces an adjustment between mass and motion fields to accommodate the new information. Inevitable by-products of this adjustment are gravitational oscillations, which have been termed "shocks." These oscillations can be of sufficient amplitude to reduce or destroy the usefulness of the assimilation system, and so must be dissipated as promptly as possible. A great deal of attention has been devoted to the problem of effective damping of these shocks.

Several methods have been proposed, ranging from avoiding the problem by employing a balanced model (Bengtsson and Gustavsson, 1971) to incorporating special viscosity terms which damp the divergent component of the wind without affecting the vorticity (Sadourny, 1972). Another method which has been used extensively is the Euler-backward time integration method (e.g., Talagrand, 1972). Morel has argued that the use of special viscosity terms is superior because of their greater selectivity. It might be added that they are far less expensive than the Euler-backward method.

The present note examines yet another method of damping the gravitational shocks resulting from direct insertion of asynoptic observations into a primitive-equation model. It is called the "implicit-backward" time integration method and was apparently first suggested by Marchuk in the early 1960's. A rather detailed account of the method may be found in Marchuk (1965). In this country, Kurihara (1965) performed a linear analysis of this and other explicit and implicit methods, and concluded that although it effectively damps gravitational oscillations, it is weakly unstable with respect to the meteorological modes. However, he found that the amplification rate is very small and suggested that the method is suitable for short-range, but not for extended-range predictions.

The four-dimensional data assimilation problem may be thought of as a series of short-period forecasts in which it is essential to damp gravitational oscillations without affecting the meteorological modes. The implicit-backward method therefore seems admirably suited for the task.

In the next section, a linear analysis of the method as applied to the gravity-wave equations is performed and response curves showing the damping characteristics are presented. The third section describes a series of experiments with a primitive-equation barotropic model and four integration methods, designed to yield a comparison of the effectiveness of the implicit-backward as opposed to other methods. Finally, in the last section are given a summary and an outline of future experiments in four-dimensional data assimilation with the implicit-backward method.

II. Linear Analysis and Response of the Implicit-Backward Method

The implicit-backward method will be applied to the equations governing one-dimensional flow of a homogeneous fluid of mean depth H, imbedded in a mean current U. The differential equations are

$$\frac{\partial u}{\partial t} + \frac{\partial \phi}{\partial x} + U\frac{\partial u}{\partial x} = 0 \tag{1}$$

$$\frac{\partial \phi}{\partial t} + c^2\frac{\partial u}{\partial x} + U\frac{\partial \phi}{\partial x} = 0 \tag{2}$$

where u is the velocity component in the x-direction, $\phi = gh$ is the geopotential perturbation from the mean gH, and $c = \sqrt{gH}$ is the phase speed of the gravity wave when U = 0. It will be assumed for the moment that the spatial behavior is trigonometric, so that the spatial derivatives are known. The finite-difference analogues of eqns. (1) and (2) are

$$u^{n+1} - u^{n-1} + 2\Delta t\ \phi_x^{n\,n+1} + 2U\Delta t\ u_x^n = 0 \tag{3}$$

$$\phi^{n+1} - \phi^{n-1} + 2\Delta t\ c^2 u_x^{n+1} + 2U\Delta t\ \phi_x^n = 0\ , \tag{4}$$

in which the superscript "n" denotes the time level, $t = n\Delta t$. Centered finite differences have been employed to approximate the temporal derivatives. It will be observed that this system is the usual "leap-frog" scheme with respect to the advection terms, which are calculated explicitly. The implicit character of the system arises because the geopotential-gradient term in eqn. (3) and the divergence term in eqn. (4) are evaluated at time $t = (n+1)\Delta t$. The term "backward" in the nomenclature is due to the fact that this system (with $U = 0$) is the reverse of the "forward" integration method in which these two terms are evaluated at $t = (n-1)\Delta t$. It is noteworthy that (again for $U = 0$), just as the forward method is amplifying and therefore absolutely unstable, the backward method is damping and absolutely stable.

To continue with the analysis, solutions of the form

$$u = u_o \chi^n e^{ikx} \quad , \quad \phi = \phi_o \chi^n e^{ikx}$$

are assumed, where χ represents the time-dependent part of the solution. For stability, $|\chi| \leq 1$. Substitution of these forms into eqns. (3) and (4) yields, after some manipulation, the frequency equation

$$(1 \mp 2ikc\Delta t)\chi^2 + (2ikU\Delta t)\chi - 1 = 0 \tag{5}$$

which, although a quadratic in χ, is not straightforward in solution. Additional manipulation of eqn. (5) produces the intractable-appearing expression

$$\chi^2 + \left\{\frac{\mp 4\beta^2 R \sin^2 k\Delta x}{1+(2\beta \sin k\Delta x)^2} + i\frac{2\beta R \sin k\Delta x}{1+(2\beta \sin k\Delta x)^2}\right\}\chi$$

$$+ \left\{\frac{-1}{1+(2\beta \sin k\Delta x)^2} \mp i\frac{2\beta 2\beta \sin \Delta k\Delta x}{1+(2\beta \sin k\Delta x)^2}\right\} = 0 \ , \tag{6}$$

where the wave number k has been replaced by $k' = (\sin k\Delta x)/\Delta x$ to account for the effect of employing centered space differences, and the notation

$$\beta = \frac{c\Delta t}{\Delta x}$$

$$R = U/c$$

has been introduced. For the special case of $U = 0$, eqn. (6) becomes

$$\chi^2 - \frac{1}{(1+2\beta \sin k\Delta x)^2} = 0 \tag{7}$$

or

$$|\chi| = \frac{1}{1+2\beta \sin k\Delta x} \ , \tag{8}$$

which is always less than unity except when $k\Delta x = 0$ or π. The response is inversely proportional to β, so that the waves of greatest phase speed are damped most strongly. Viewed in another way, for a given phase speed, the damping rate may be increased by increasing Δt or decreasing Δx. Aside from this special case, however, eqn. (6) is so complicated that interpretation is rendered difficult. Accordingly, numerical solutions for the magnitude of χ have been calculated, as a function of wavelength, and for several values of β and R. Eqn. (6) is of the form

$$\chi^2 + (A+iB)\chi + (C+iD) = 0$$

for which Kurihara (1965) gives the solutions. Kurihara's formulae have been employed here. The results are displayed in Figure 1. It should be noted that there are four roots of eqn. (6). In the diagram, only one is displayed for $U/c = 0$, the remaining three having identical values of $|\chi|$. For $U/c \neq 0$, two roots are plotted, the remaining two being identical.

The diagram indicates that, for $U/c = 0$, the greatest damping occurs for the $4\Delta x$ wave and increases with increasing β. As U/c increases, the damping rate increases for one root and decreases for the other. At $U/c = 1$, one root is heavily damped, the other neutral. For $U/c > 1$, one root becomes unstable.

It may therefore be concluded that the backward implicit is conditionally stable with respect to gravitational modes so long as $U/c \leq 1$, and that the scheme is strongly damping. This is in agreement with Kurihara's analysis. It suggests that the method is suitable for damping gravitational oscillations, since U/c is very nearly always less than unity except for some of the lower internal modes in a multilevel model. The present analysis, however, is not directly applicable to such modes.

No attempt is made here to duplicate or extend Kurihara's analysis of the implicit-backward method where meteorological modes are present. Instead, the next section presents experimental evidence which confirms Kurihara's conclusions.

III. Experimental Results

A series of 48-hour forecasts from real initial data were conducted with a primitive-equation barotropic model. Four different time integration techniques were employed: the "leapfrog" (explicit-neutral), the Euler-backward (explicit-damping), an implicit-neutral method previously utilized by the author (McPherson, 1971), and the implicit-backward method. The domain of the model is a quasi-hemispheric rectangle on a polar stereographic projection of the Northern Hemisphere. The grid lattice is a 27 by 29 array of points separated by 762 km at 60N. Wind components, u and v, are defined at the center of grid boxes, while the geopotential ϕ is defined at grid points. This

arrangement of history variables has previously been used by Kwizak and Robert (1971) and McPherson. The lateral boundary specifications are such that geopotentials are kept invariant with time at the outer row of grid points, and the velocity components are invariant with time at the outer row of grid boxes.

Initial data were the same for all experiments. Analyzed 500 mb heights were obtained for 12Z February 1, 1969, from which geostrophic winds were calculated. The small divergence remaining in the resulting wind field was removed, and the nondivergent winds were used to invert the balance equation to obtain a height field to balance the motion field. Nevertheless, a residual imbalance remained, producing small but noticeable gravitational oscillations. The initial fields of height, velocity, divergence, and vorticity are shown in Figures 2-5.

The finite-difference equations have the form

$$\overline{u}_t^t + 2\Delta t\, \overline{\phi}_x^y = 2\Delta t \left\{ f_o v + \overline{\overline{v}^{xy}(f' + \zeta) - \overline{K}_x^y}^{xy} \right\} \equiv U \tag{9}$$

$$\overline{v}_t^t + 2\Delta t\, \overline{\phi}_y^x = 2\Delta t \left\{ f_o u - \overline{\overline{u}^{xy}(f' + \zeta) - \overline{K}_y^x}^{xy} \right\} = V \tag{10}$$

$$\overline{\phi}_t^t + 2\Delta t\, m^2 c^2 \left(\overline{u}_x^y + \overline{v}_y^x\right) = 2\Delta t \left\{ -m^2 \left(\overline{(\overline{u}^{xy}\phi)_x^y + (\overline{v}^{xy}\phi)_y^x}^{xy} \right) \right\} = Z \tag{11}$$

where the velocity components are scaled by the map factor m, and

$\zeta = m^2\left(\overline{v}_x^y - \overline{u}_y^x\right)$,

$K = \frac{1}{2}\left\{(mu)^2 + (mv)^2\right\}$

f_o = coriolis parameter at 45N,

f' = deviation of coriolis parameter from f_o,

$c = \sqrt{gH}$, H = mean depth of the fluid.

The averaging and differencing notation is standard:

$$\psi_x = \frac{1}{\Delta x}\left\{\psi\left(x + \frac{\Delta x}{2}\right) - \psi\left(x - \frac{\Delta x}{2}\right)\right\}$$

$$\overline{\psi}^x = \frac{1}{2}\left\{\psi\left(x + \frac{\Delta x}{2}\right) + \psi\left(x + \frac{\Delta x}{2}\right)\right\}.$$

The right-hand sides of eqns. (9-11) are evaluated identically in each experiment, using values at the current time, $t = n\Delta t$. The difference between the explicit and implicit schemes lies in the treatment of the second term on the left side of each equation. Specifically, the forms for each method are:

Leapfrog (explicit-neutral)

$$\overline{u}_t^t = U - 2\Delta t\left(\overline{\phi}_x^y\right)^n \tag{12}$$

$$\overline{v}_t^t = V - 2\Delta t\left(\overline{\phi}_y^x\right)^n \tag{13}$$

$$\overline{\phi}_t^t = Z - 2\Delta t\ m^2c^2(\overline{u}_x^y + \overline{v}_y^x)^n \tag{14}$$

Euler-backward (explicit-damping)

$$u^* = u^n + \tfrac{1}{2}U - \Delta t(\overline{\phi}_x^y)^n \tag{15}$$

$$v^* = v^n + \tfrac{1}{2}V - \Delta t(\overline{\phi}_y^x)^n \tag{16}$$

$$\phi^* = \phi^n + \tfrac{1}{2}Z - \Delta t\ c^2m^2(\overline{u}_x^y + \overline{v}_y^x)^n \tag{17}$$

$$u^{n+1} = u^n + \tfrac{1}{2}U^* - \Delta t(\overline{\phi}_x^y)^* \tag{18}$$

$$v^{n+1} = v^n + \tfrac{1}{2}V^* - \Delta t(\overline{\phi}_y^x)^* \tag{19}$$

$$\phi^{n+1} = \phi^n + \tfrac{1}{2}Z^* - \Delta t\ c^2m^2(\overline{u}_x^y + \overline{v}_y^x)^* \tag{20}$$

where the asterisk notation in (18-20) indicates that the calculations are done using the variables calculated in (15-17).

Implicit-neutral

$$\overline{u}_t^t + \Delta t\left(\overline{\phi^{n+1} + \phi^{n-1}}\right)_x^y = U \tag{21}$$

$$\overline{v}_t^t + \Delta t\left(\overline{\phi^{n+1} + \phi^{n-1}}\right)_y^x = V \tag{22}$$

$$\overline{\phi}_t^t + \Delta t\ c^2m^2\left[\left(\overline{u}_x^y + \overline{v}_y^x\right)^{n+1} + \left(\overline{u}_x^y + \overline{v}_y^x\right)^{n-1}\right] = Z \tag{23}$$

Implicit-damping

$$\overline{u}_t^t + 2\Delta t\left(\overline{\phi}_x^y\right)^{n+1} = U \tag{24}$$

$$\overline{v}_t^t + 2\Delta t\left(\overline{\phi}_y^x\right)^{n+1} = V \tag{25}$$

$$\overline{\phi}_t^t + 2\Delta t\ m^2c^2\left(\overline{u}_x^y + \overline{v}_y^x\right)^{n+1} = Z \tag{26}$$

Both explicit versions used Δt = 10 minutes, and both implicit versions used Δt = 1 hour.

The results of the four 48-hour forecasts are shown in Figures 6-9. We have chosen to illustrate the experiments in terms of the time variation of the total kinetic energy (KE), the root-mean-square (RMS) value of the height departure (Z_d), the RMS vorticity (ζ), and the RMS divergence ($\nabla\cdot\vec{V}$). Each curve has, for reference, the appropriate curve from the explicit-neutral experiment.

Figure 6 shows the behavior of the RMS height departure. The variations in the explicit-neutral curve indicate the presence of a fairly large-amplitude gravity wave with a relatively long period, about 18 hours. This oscillation is damped to some extent by the Euler-backward method. The implicit-neutral method displays no damping, of course, and is very similar in all but fine detail to the explicit-neutral method. The differences that do exist are probably due to time-truncation error.

The implicit-backward scheme displays pronounced damping of this oscillation, such that it is nearly indistinguishable by 48 hours. An undesirable feature is the tendency for separation of solutions on odd- and even-numbered time steps. This difficulty was overcome by the introduction of a light time-filter (Asselin, 1971; Gerrity and Scolnik, NMC Office Note 62) applied to each history variable. The result is shown in the lowest curve of Figure 6. It is evident that the temporal computational mode has been eliminated.

Figure 7 illustrates the kinetic energy. The 18-hour oscillation is evident in this parameter, also. Once again, the implicit-backward exhibits superior damping response compared to the Euler-backward. This conclusion is more strikingly apparent in the RMS divergence, shown in Figure 8.

Figures 6-8 demonstrate that the implicit-backward is superior to the Euler-backward in terms of the damping of gravitational oscillations. One remaining concern is the treatment of the meteorological modes, since Kurihara has demonstrated a weak instability of the implicit-backward with respect to these modes. Figure 9 displays the RMS vorticity from the various experiments. The implicit-backward curve, without the time filter, shows the presence of the temporal computational mode. Introducing the filter removes this noise, and leaves intact a curve which compares favorably to the explicit-neutral curve. There is no discernible evidence of a faster growth rate of vorticity with the implicit backward.

Finally, Figures 10-13 show the 48-hour forecasts from the implicit-backward. All fields are well-behaved. It is especially noteworthy that the divergence is very small in magnitude and large in scale, while the vorticity pattern, except for translation, is virtually unchanged.

IV. Future Plans

This effort is a first step toward development of an operational continuous four-dimensional data assimilation system. The effectiveness of the implicit-backward technique as an economical device for damping gravitational oscillations has been demonstrated. Further research will involve (1) simulated four-dimensional data assimilation experiments along the outlines of Talagrand's work, and (2) an investigation of the behavior of the implicit-backward technique in the multilevel model now being tested at NMC. Should the latter experiments indicated demonstrate that the implicit-backward is an effective method of damping gravitational oscillations in a multilevel model, the next step will be data assimilation experiments with that model. Subsequent research should involve continuous assimilation experiments with an implicit version of the NMC eight-layer global model.

REFERENCES

Asselin, R., 1972: "A frequency filter for time integrations," Monthly Weather Review, Vol. 100, No. 6.

Bengtsson, L., and N. Gustavsson, 1971: "An experiment in the assimilation of data in dynamical analysis," Tellus, Vol. 23, No. 4-5.

Gerrity, J., and S. Scolnik, 1971: "Some comments on Robert's time filter for time integration," NMC Office Note 62.

Kurihara, Y., 1965: "On the use of implicit and iterative methods for the time integration of the wave equation," Monthly Weather Review, Vol. 93, No. 1.

Kwizak, M., and A. Robert, 1971: "A semi-implicit scheme for grid point atmospheric models of the primitive equations," Monthly Weather Review, Vol. 99, No. 1.

Marchuk, G., 1965: Numerical Methods for Solving Weather-Forecasting and Climate-Theory Problems Part I. Translated from Russian by American Meteorological Society for Air Force Cambridge Research Laboratory.

McPherson, R., 1971: "Note on the semi-implicit integration of a fine-mesh, limited-area prediction model on an off-set grid," Monthly Weather Review, Vol. 99, No. 3.

Morel, P., and O. Talagrand, 1972: "The dynamic approach to meteorological data assimilation," unpublished manuscript, Laboratoire Météorologie Dynamique, Ecole Normale Supérieure, Paris.

Sadourny, R., 1972: "Forced geostrophic adjustment in large scale flow," Laboratoire de Météorologie Dynamique du C.N.R.S., Paris, unpublished manuscript.

Talagrand, O., 1972: "On the damping of high-frequency motions in four-dimensional assimilation of meteorological data," Journal of the Atmospheric Sciences, Vol. 29, No. 8.

LIST OF FIGURES

1. Damping characteristics of the implicit-backward method applied to the gravity wave equations. The magnitude of the time-dependent part of the solution is plotted as the ordinate against wave number or wavelength in abscissa, for several values of the stability ratio $\beta = c\Delta t/\Delta x$ and the ratio U/c.

2. Initial 500 mb height in meters for 12Z February 1, 1969. For reference, the 30° latitude circle and the 80th meridian are indicated.

3. Initial velocity field for 12Z February 1, 1969. Units are m sec^{-1}.

4. Initial divergence field for 12Z February 1, 1969. Units are 10^{-7} sec^{-1}.

5. Initial vorticity field for 12Z February 1, 1969. Units are $10^{-7}sec^{-1}$.

6. Temporal variation of the RMS height departure in meters from the mean height of the 500 mb surface. The solid line in each graph is produced by the explicit-neutral model. Dashed lines: top graph, explicit-damping; second graph, implicit-neutral; third graph, implicit-damping without time filter; fourth graph, implicit-damping with time filter.

7. Temporal variation of the total kinetic energy. Solid and dashed lines as in Figure 6.

8. Temporal variation of RMS divergence in units of $10^{-8}sec^{-1}$. Solid and dashed lines as in Figure 6.

9. Temporal variation of RMS vorticity in units of $10^{-8}sec^{-1}$. Solid and dashed lines as in Figure 6.

10. 48-hour 500-mb height forecast from implicit-backward model.

11. 48-hour 500 mb velocity forecast from implicit-backward model.

12. 48-hour 500 mb divergence forecast from implicit-backward model.

13. 48-hour 500 mb vorticity forecast from implicit-backward model.

ROOT 1 ROOT 2

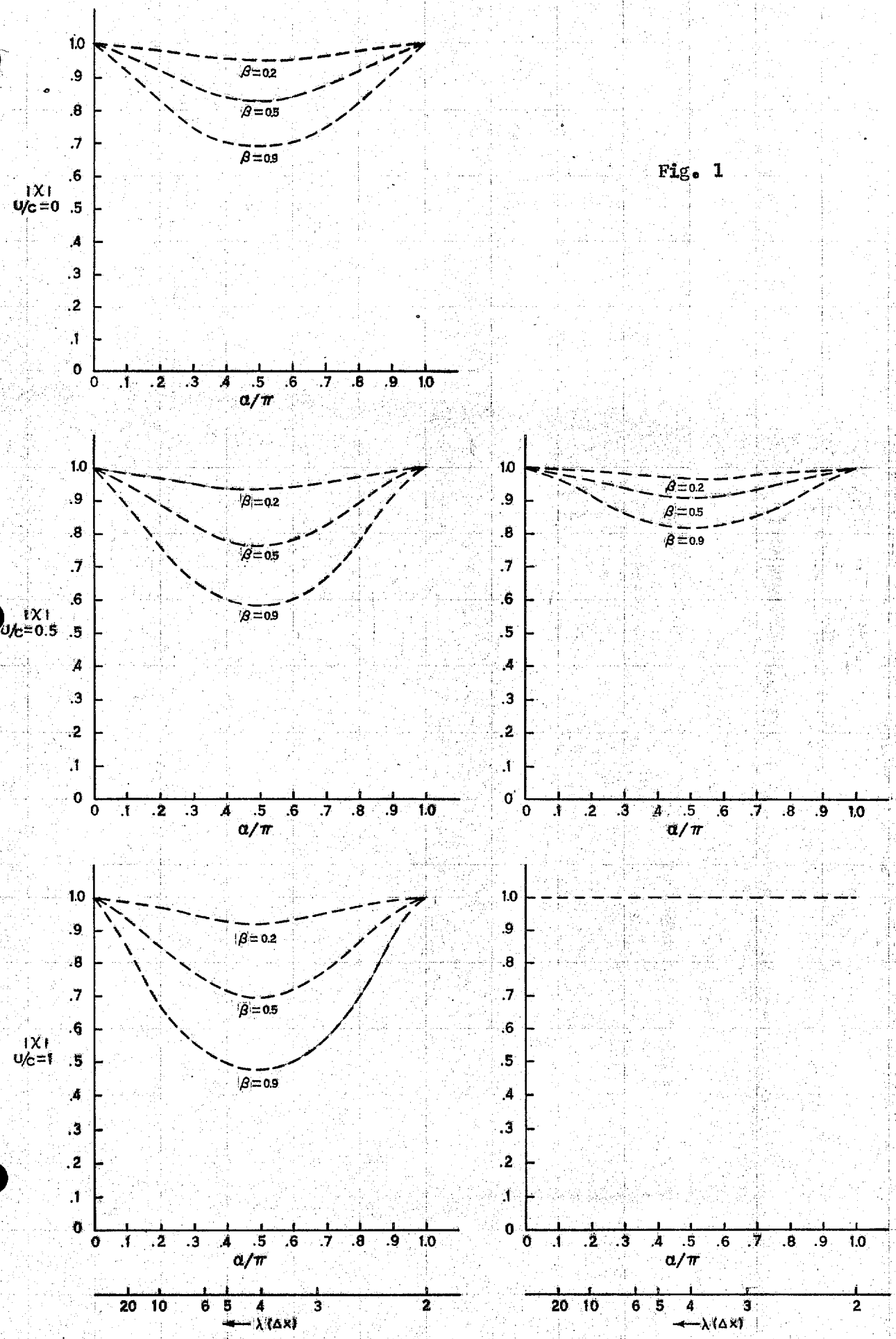

Fig. 1

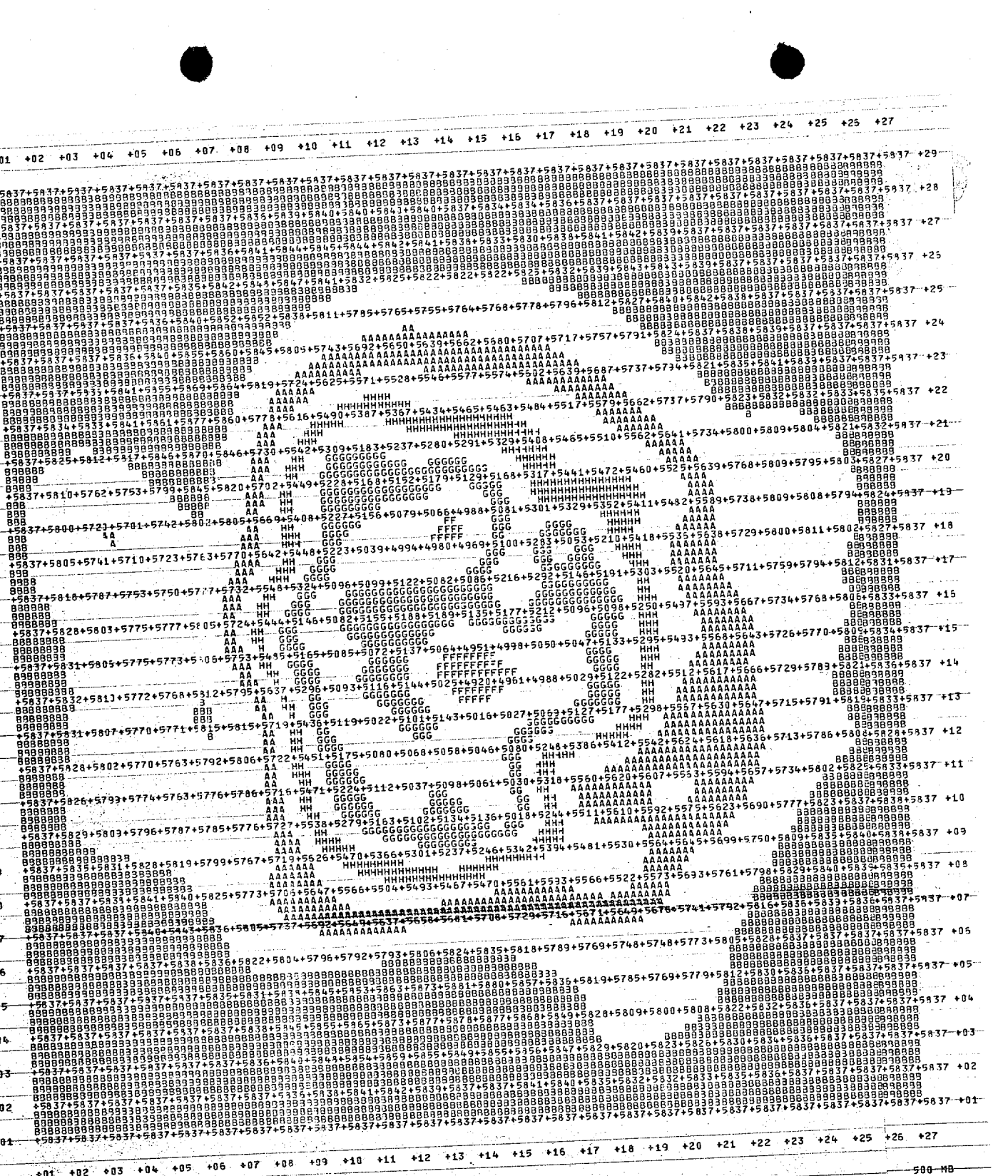

Figure 2.

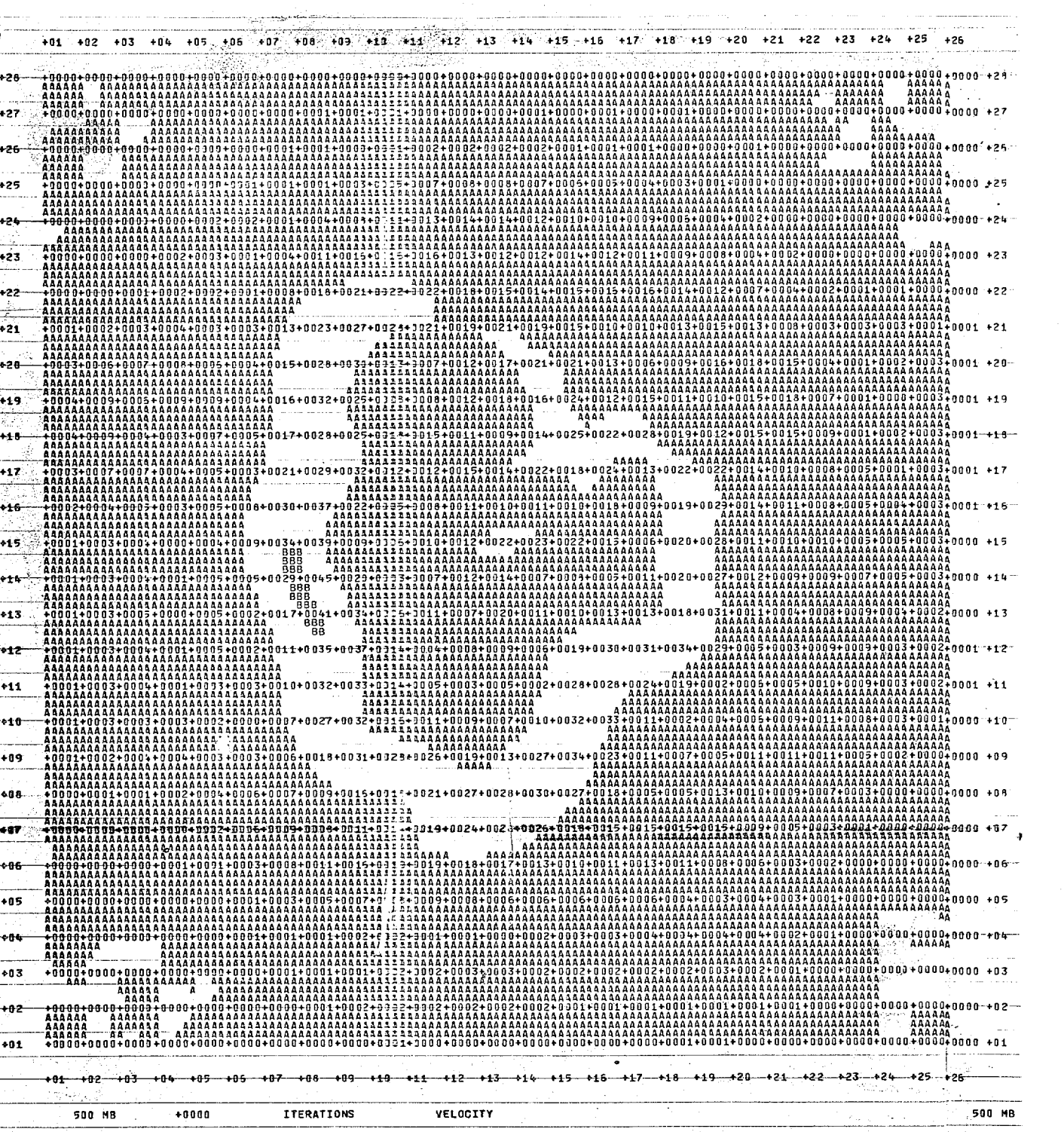

Figure 3.

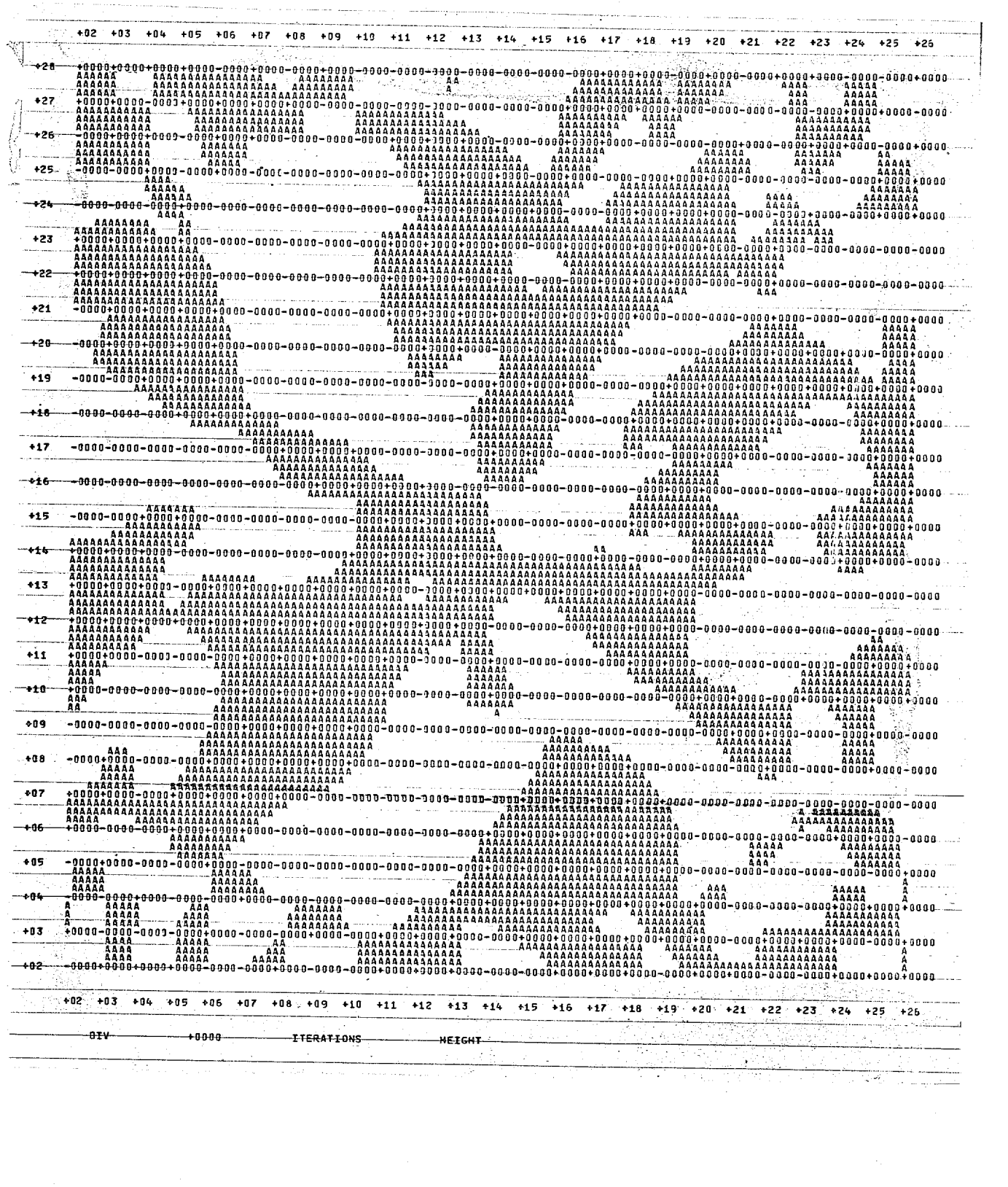
+02 +03 +04 +05 +06 +07 +08 +09 +10 +11 +12 +13 +14 +15 +16 +17 +18 +19 +20 +21 +22 +23 +24 +25 +26
+28
+27
+26
+25
+24
+23
+22
+21
+20
+19
+18
+17
+16
+15
+14
+13
+12
+11
+10
+09
+08
+07
+06
+05
+04
+03
+02
+02 +03 +04 +05 +06 +07 +08 +09 +10 +11 +12 +13 +14 +15 +16 +17 +18 +19 +20 +21 +22 +23 +24 +25 +26
DIV
+0000
ITERATIONS
HEIGHT

Figure 4.

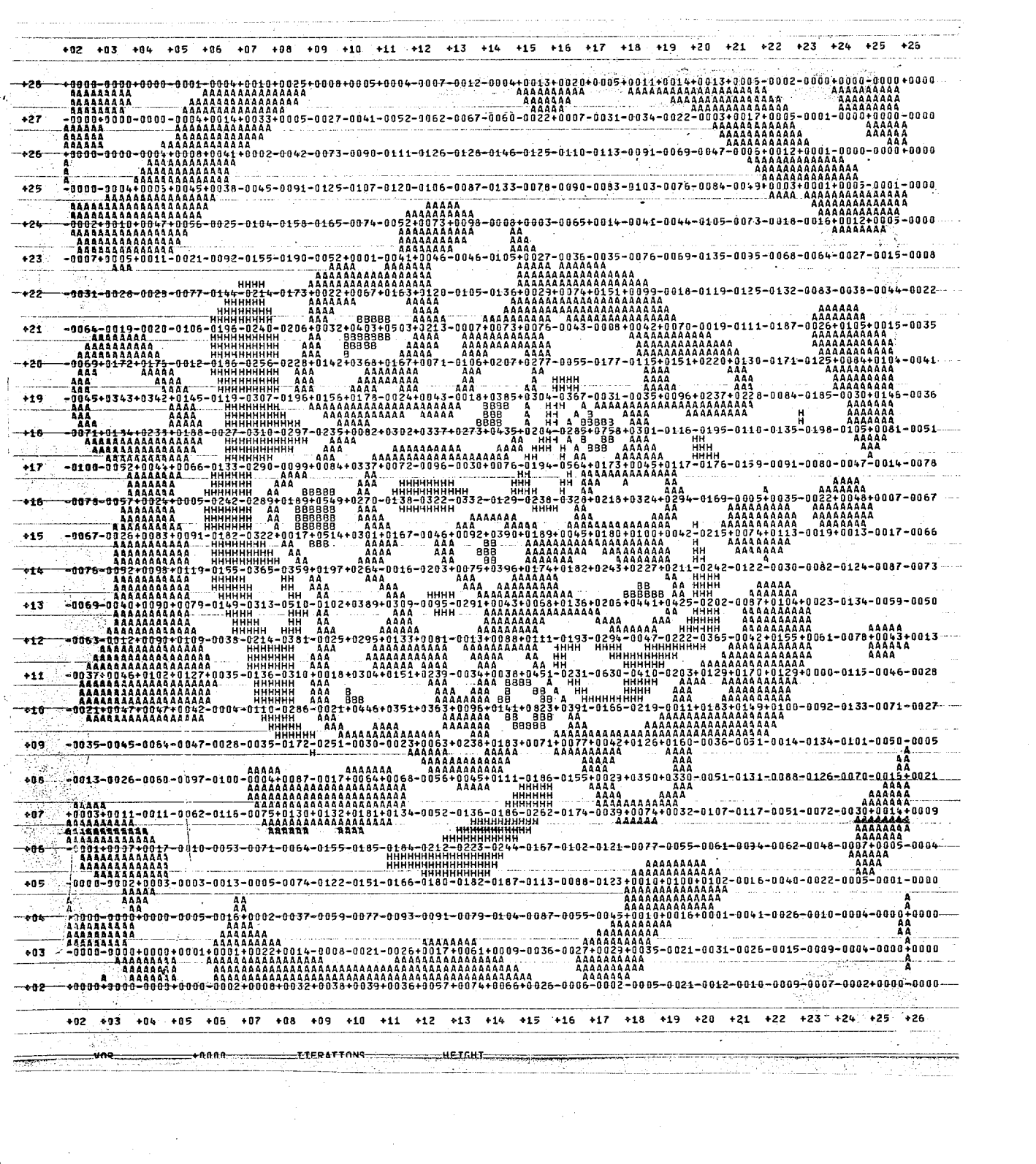

Figure 5.

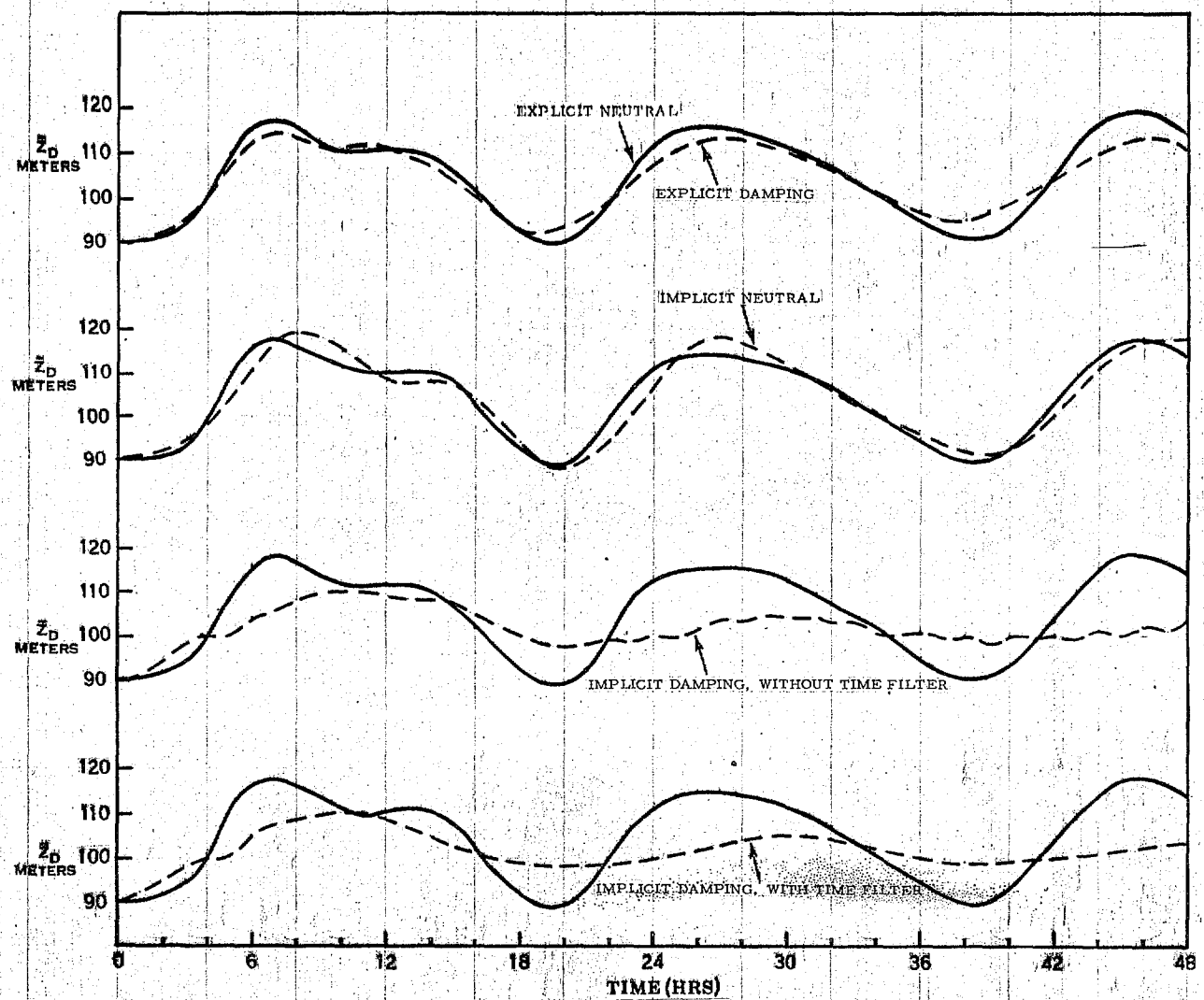
EXPLICIT NEUTRAL
EXPLICIT DAMPING
IMPLICIT NEUTRAL
IMPLICIT DAMPING, WITHOUT TIME FILTER
IMPLICIT DAMPING, WITH TIME FILTER
$\tilde{z}_D$ METERS
120
110
100
90
0
6
12
18
24
30
36
42
48
TIME (HRS)

FIG. 6

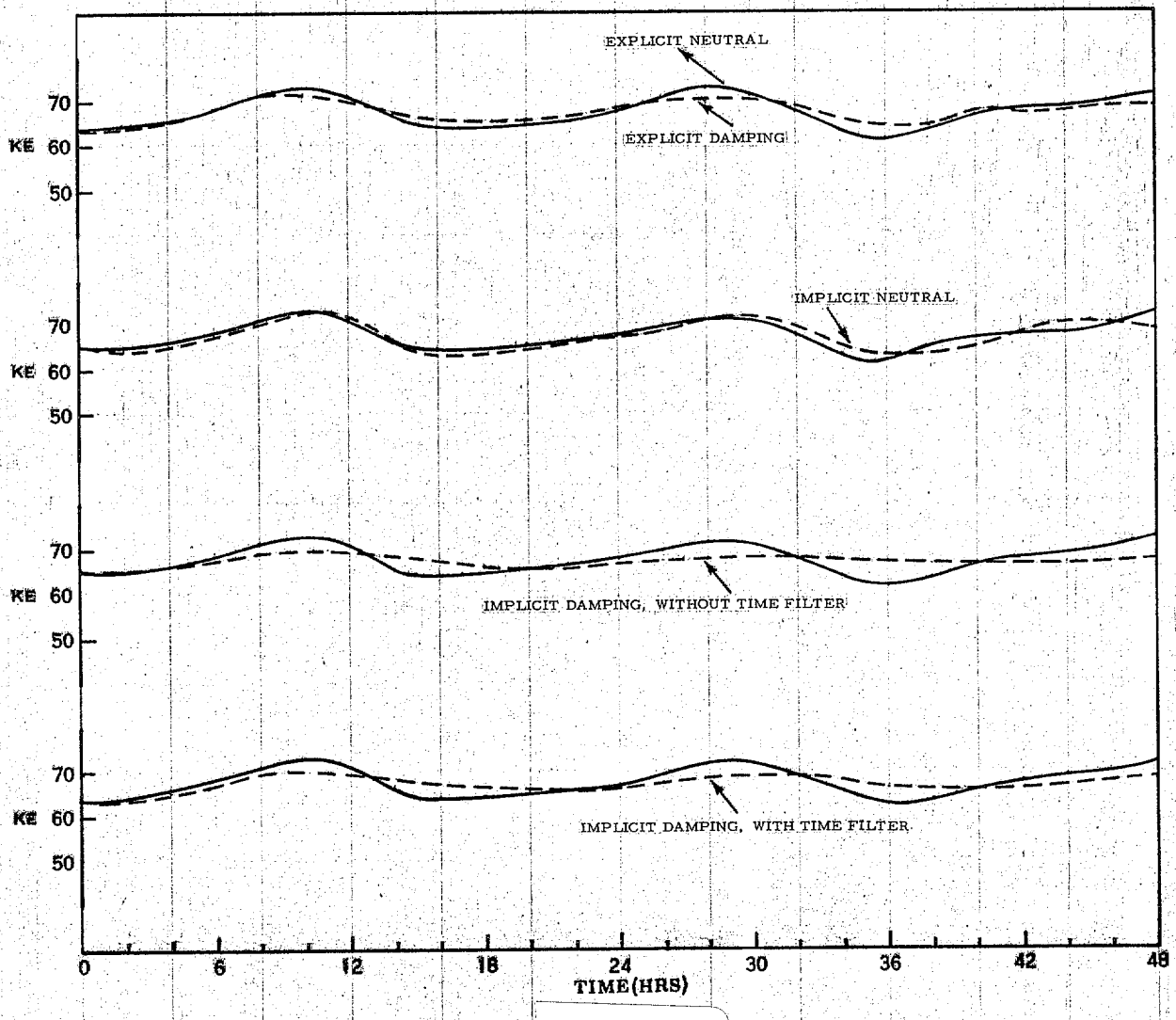
EXPLICIT NEUTRAL
EXPLICIT DAMPING
IMPLICIT NEUTRAL
IMPLICIT DAMPING, WITHOUT TIME FILTER
IMPLICIT DAMPING, WITH TIME FILTER
KE
70
60
50
0
6
12
18
24
30
36
42
48
TIME(HRS)

FIG. 7

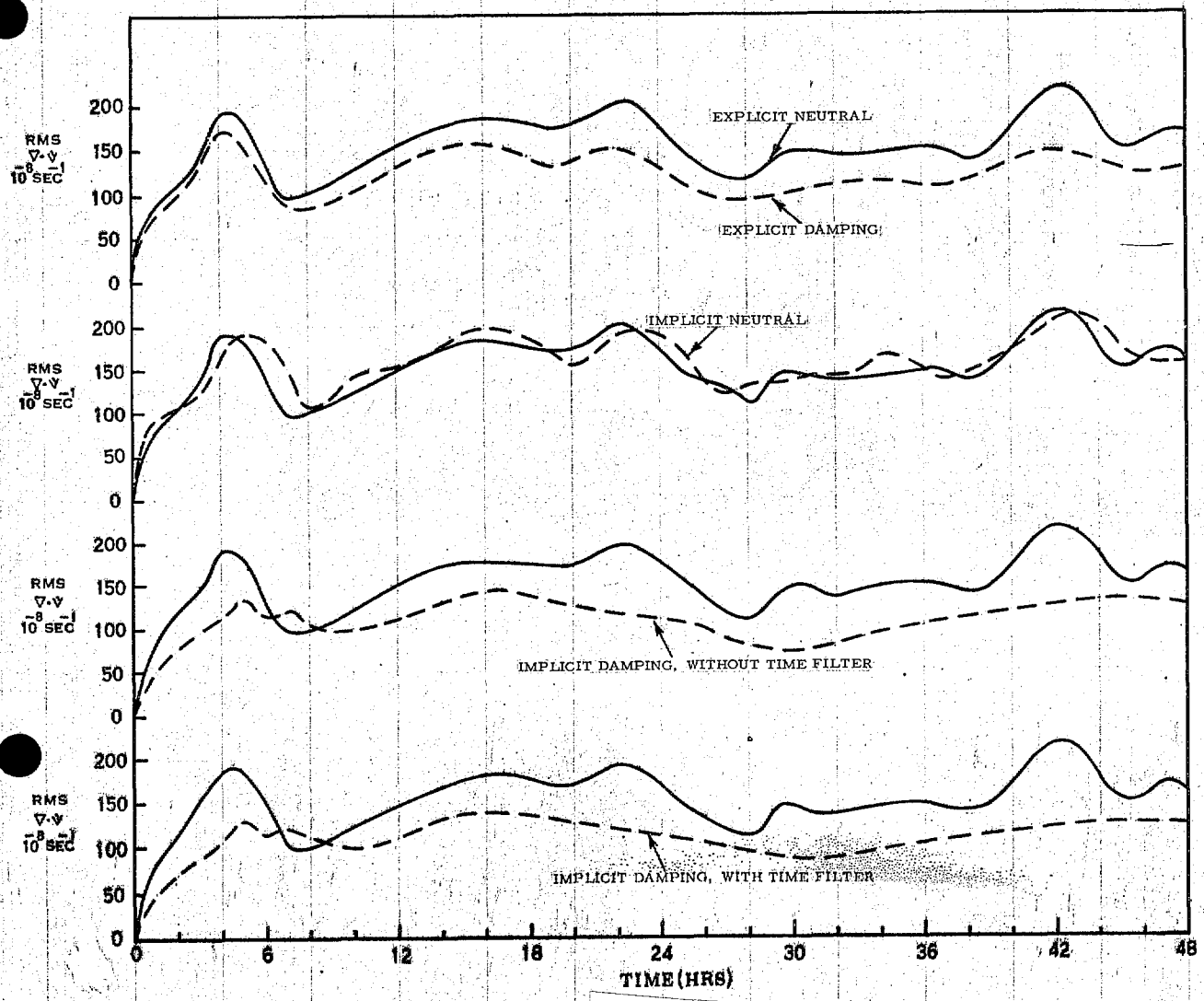
RMS
$\nabla \cdot \vec{v}$
10^{-8} SEC^{-1}
200
150
100
50
0
EXPLICIT NEUTRAL
EXPLICIT DAMPING
IMPLICIT NEUTRAL
IMPLICIT DAMPING, WITHOUT TIME FILTER
IMPLICIT DAMPING, WITH TIME FILTER
0
6
12
18
24
30
36
42
48
TIME (HRS)

FIG. 8

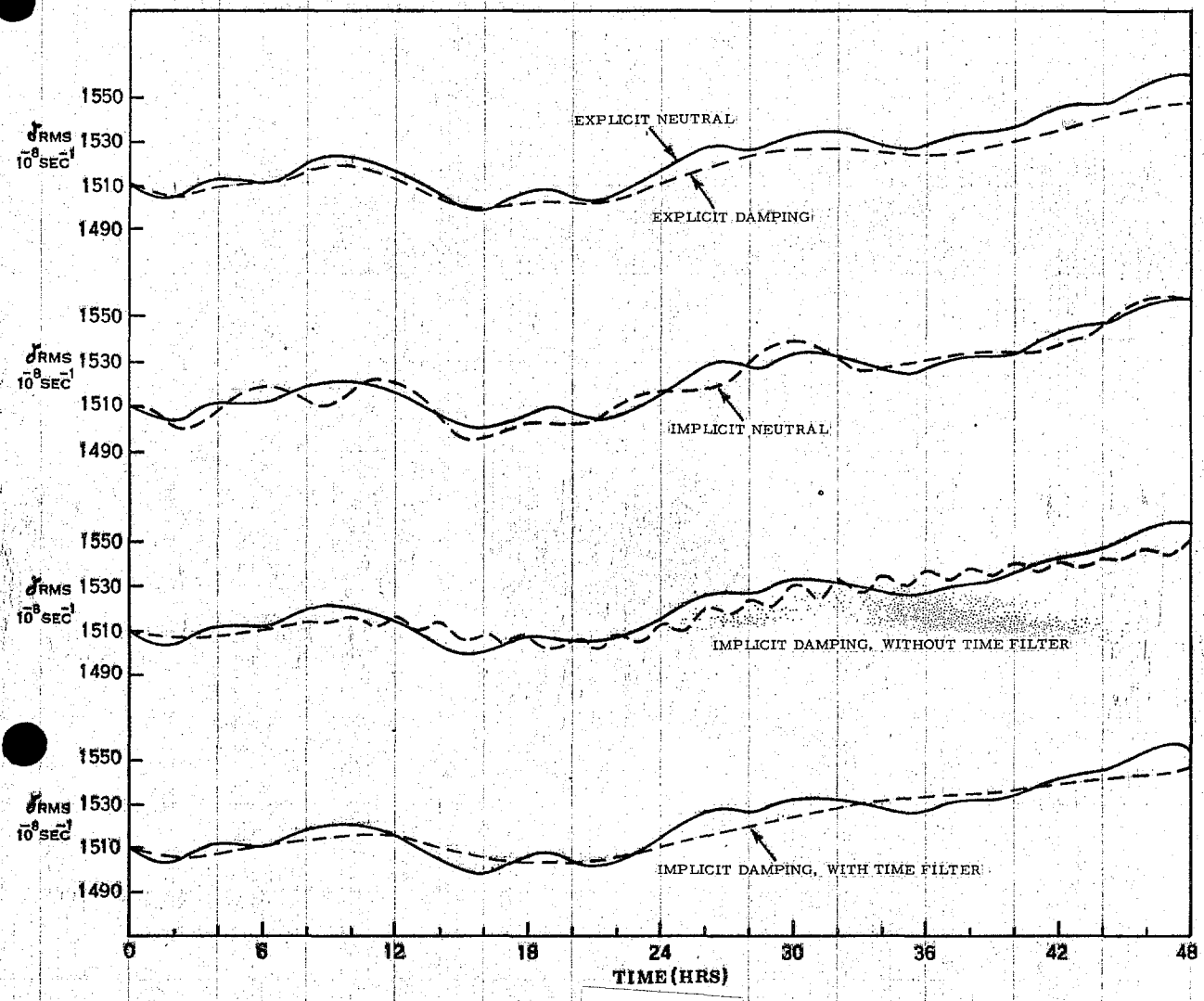
1550
1530
1510
1490
ζ_{RMS} 10^{-8} SEC^{-1}
EXPLICIT NEUTRAL
EXPLICIT DAMPING
IMPLICIT NEUTRAL
IMPLICIT DAMPING, WITHOUT TIME FILTER
IMPLICIT DAMPING, WITH TIME FILTER
0
6
12
18
24
30
36
42
48
TIME (HRS)

FIG. 9

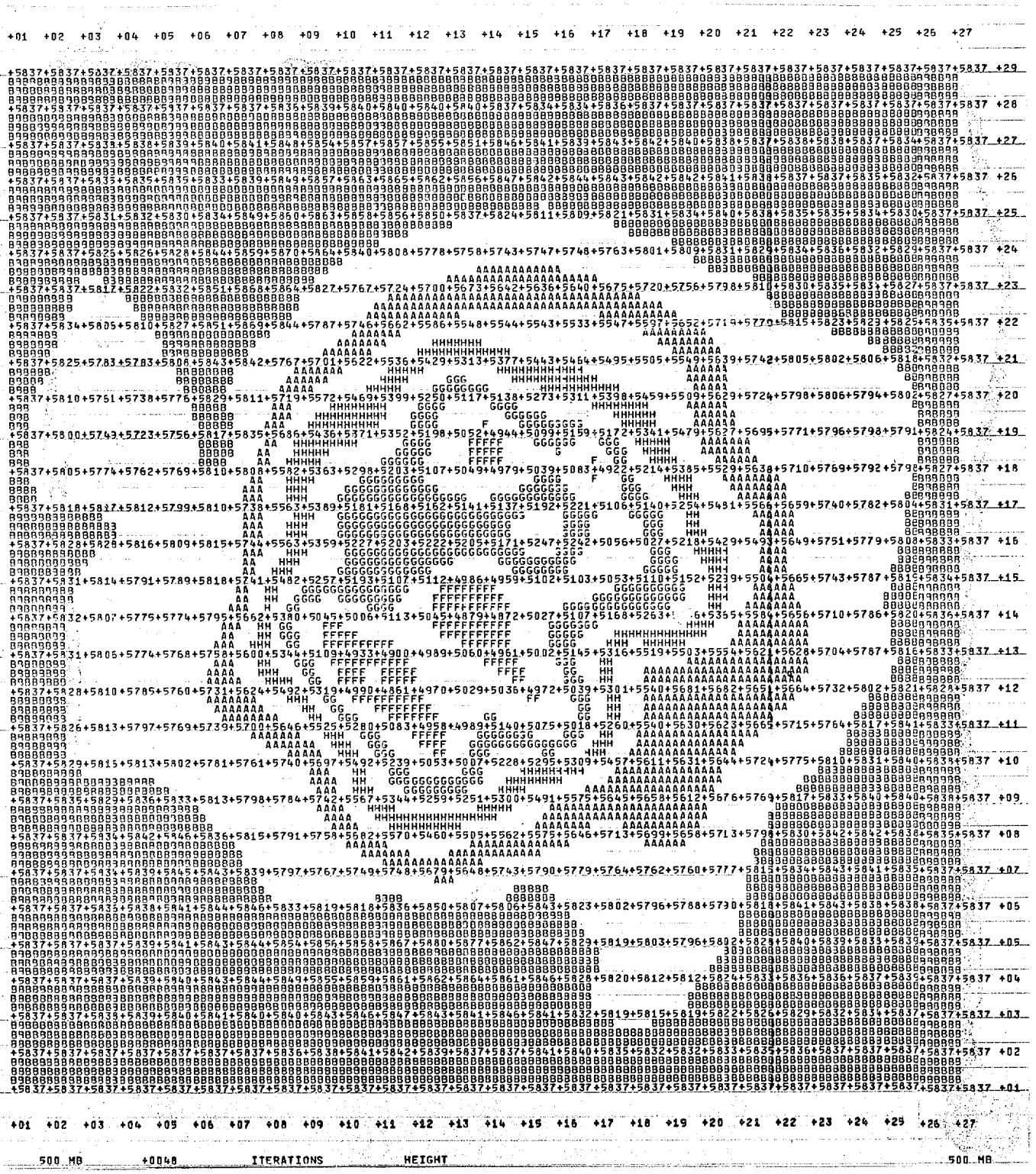

Figure 10.

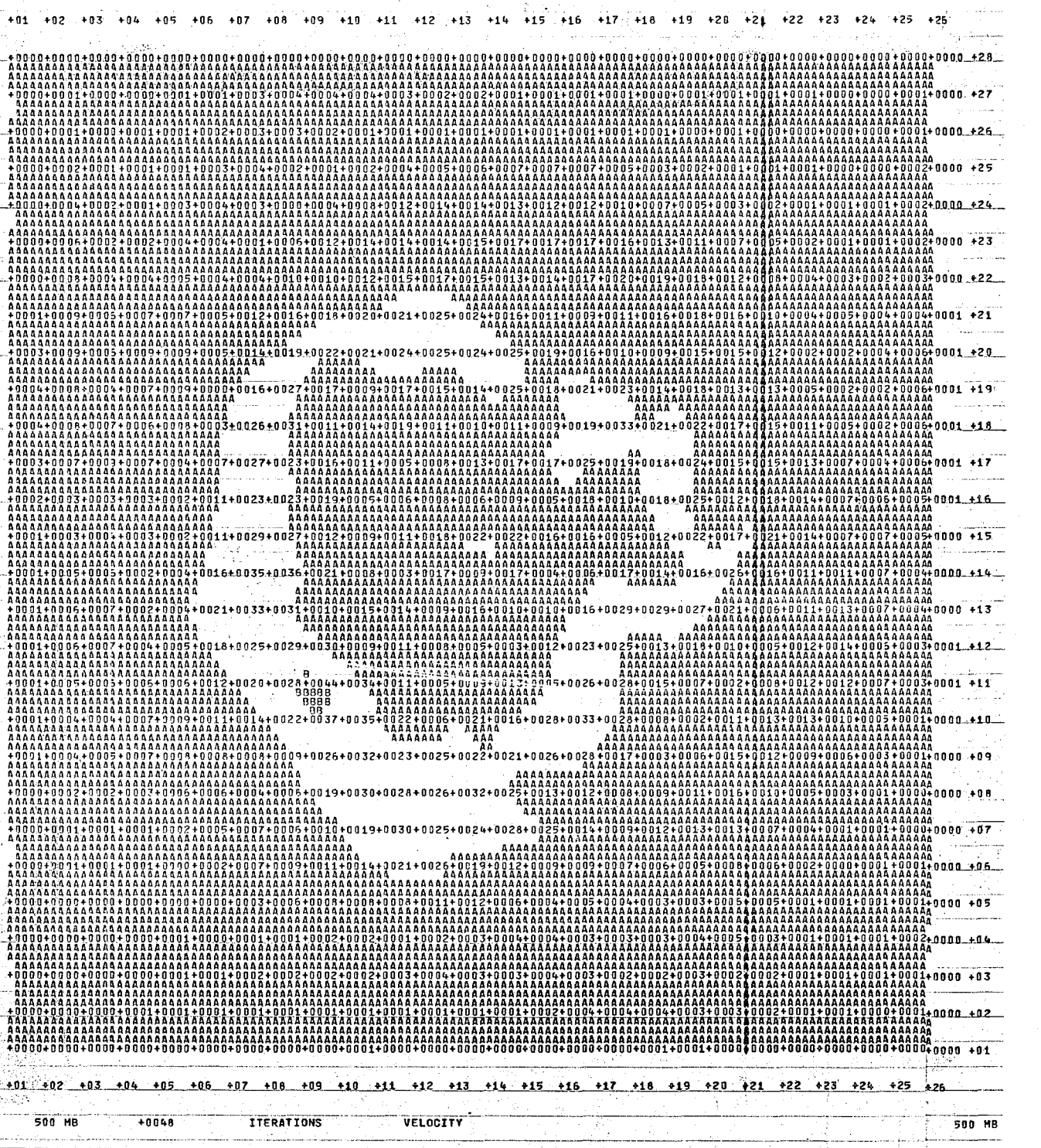

Figure 11.

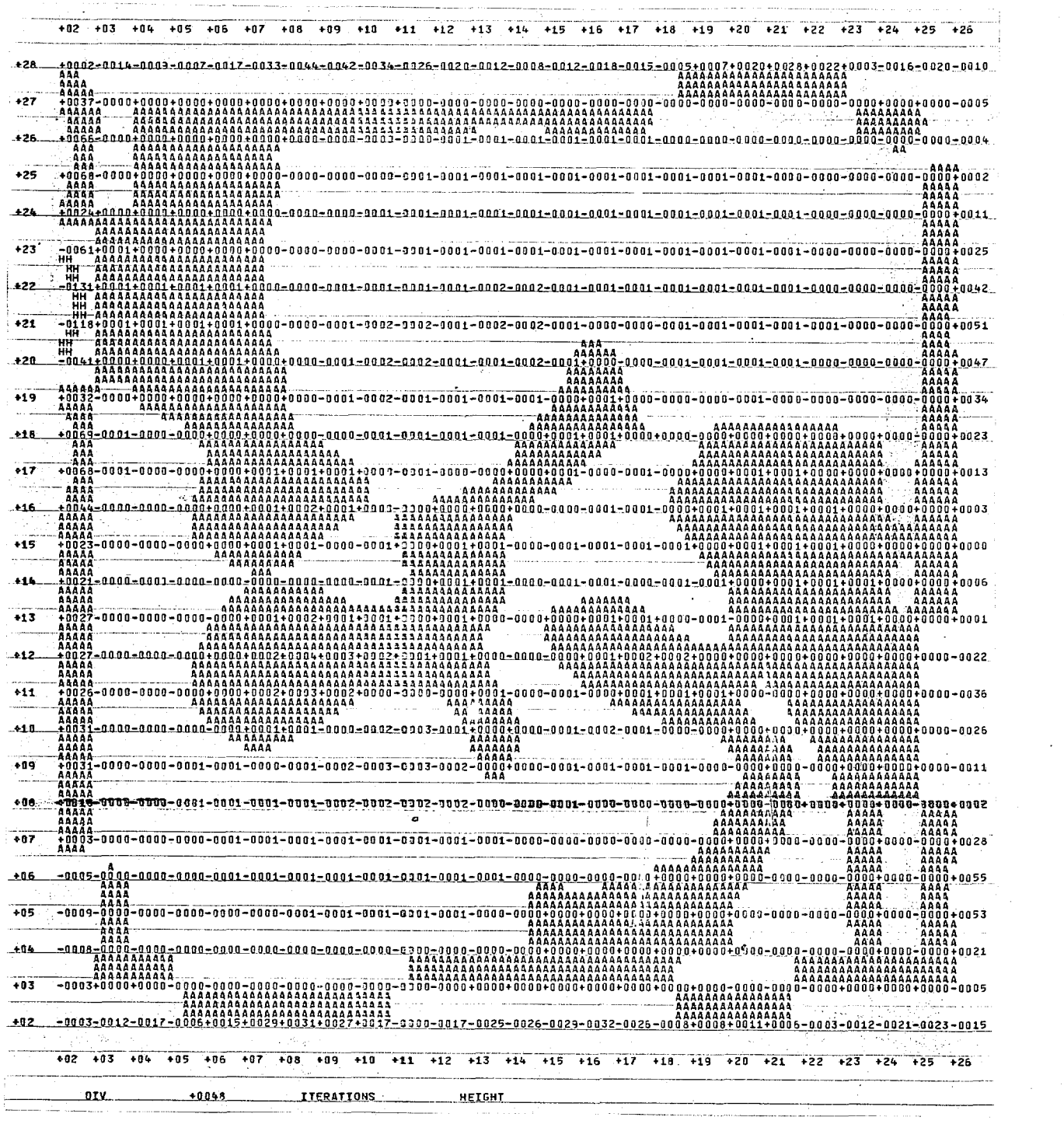

Figure 12.

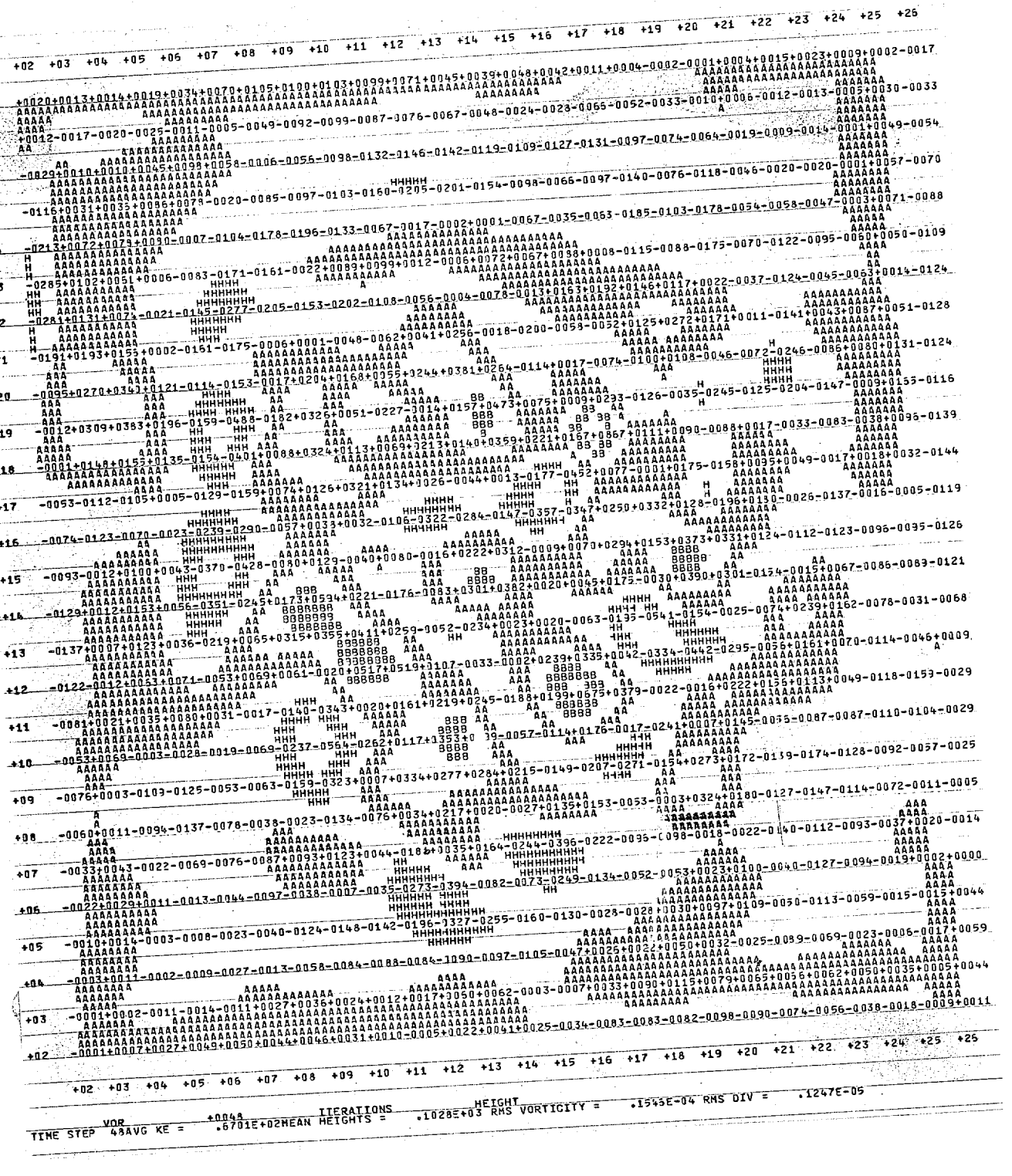

TIME STEP 48AVG KE = .6701E+02MEAN HEIGHTS = .1028E+03 RMS VORTICITY = .1545E-04 RMS DIV = .1247E-05

Figure 13.